XLVI CILAMCE
VITÓRIA - ES - BRAZIL - 2025
XLVI IBERO-LATIN AMERICAN CONGRESS ON COMPUTIONAL METHODS IN ENGENEERING

On the two-dimensional analysis of reinforced materials using the BEM/1D-BEM coupling

Mário S. O. César Filho[1], Edson D. Leonel[1]

[1]*Dept. of Structural Engineering, São Carlos School of Engineering, University of São Paulo*
Trabalhador São Carlense Ave., 13566 − 590*, São Paulo, Brazil*
mariocesarfilho@usp.br, edleonel@sc.usp.br

Abstract. The design of structures composed of different materials has become increasingly common due to the demands for economic feasibility and high performance in new projects. For evaluating the mechanical quantities of such structures, the coupling of the Boundary Element Method (BEM) with its one-dimensional version, the 1D-BEM, has shown excellent results when compared to commercial software. This coupling proves to be numerically stable in comparison to the classical one with reinforcements represented by the Finite Element Method. The BEM/1D-BEM formulation presented herein accounts perfect adherence between the matrix domain and the reinforcements. For building the global system of equations, this coupling scheme requires the integral equation for assessing the displacements in internal points, which may be computationally costly. This study proposes an efficient discretization methodology for the reinforcements, reducing the number of internal points required for evaluating the aforementioned integral. Additionally, strategies are proposed to avoid accuracy loss due to near singularities resulting from the proximity of sources in a reinforcement domain to other domains. This issue is often observed in two-dimensional analyses and is rarely avoided without proper treatment when analyzing randomly distributed reinforcements. Examples are presented using both the classical BEM formulation and the isogeometric version (IGABEM).

Keywords: BEM, 1D-BEM, reinforced structures, isogeometric analysis.

1 Introduction

With the natural development and technological progress of humanity, the complexity of engineering design has increased. To meet current performance requirements, it is essential to enhance materials in terms of their mechanical behavior. Stiffening through the combination of different materials stands out as an effective method to improve such properties. The resulting part from this combination is referred to as a composite. In engineering practice, composites appear in numerous applications. Various types of structural concrete serve as typical examples in civil construction [1]. Composites are also commonly used in ship hull structures in the naval industry and in aircraft fuselage structures in the aerospace sector [2, 3].

In the context of using the Boundary Element Method (BEM) for the mechanical analysis of composite structures, Coda, Venturini, and Aliabadi [4] formulated its coupling with the Finite Element Method (FEM) for two-dimensional static and dynamic problems within the domain of linear elasticity. In their formulation, BEM models the solid medium, while frame finite elements represent the stiffeners. The extension of this formulation to three-dimensional analyses has focused solely on soil–structure interaction problems [5, 6].

Subsequently, returning to two-dimensional applications, Coda [7] introduces nonlinearities into the BEM and treat the reinforcements with truss finite elements. Botta and Venturini [8], still under linear and elastic assumptions in the BEM, formulate a nonlinear model for the adherence loss between the matrix and the stiffener. In their formulation, truss finite elements represent the stiffeners. Later, Rocha, Venturini, and Coda [9, 10] adapt the slip formulation to frame finite elements. To this coupling, Leonel [11] implements a nonlinear elastoplastic constitutive model for the reinforcements and a crack propagation model for the matrix.

Alternatively to the BEM/FEM coupling for the analysis of reinforced domains, researchers have also explored approaches based purely on the BEM. One such approach employs the BEM subregion technique to discretize the reinforcements with behavior analogous to truss elements [12]. Leite and Venturini [13] extend this formulation to simulate reinforcements with behavior similar to beam elements. These subregion-based approaches yield numerically stable results for the reinforcement domain in comparison to those obtained through BEM/FEM

coupling. A consistent alternative approach replaces BEM subregions with linear cells to represent the reinforcements. It leads to reduced computational cost, especially in cases with a large number of fibers [14]. Beer *et al.* [15] develop a computationally efficient three-dimensional isogeometric formulation also based on subregions.

Recently, the coupling of the BEM with its one-dimensional formulation (1D-BEM) has gained prominence in this field of analysis. On this coupling formulation, Buffon [16] considers the reinforcements to behave as truss elements. Compared directly to BEM/FEM, this approach yields numerically stable results. Compared to purely FEM-based implementations, the alternative provides physically consistent outcomes. Rodrigues Neto [17] and Rodrigues Neto and Leonel [18] further develop this coupling, including adaptation to heterogeneous media, nonlinear elastoplastic behavior for reinforcements, and extension to viscoelastic problems. The expansion to three-dimensional analysis incorporates these developments alongside a bond-slip model between matrix and fiber. The 3D approach enables validation against experimental data for static analysis [19, 20]. Incorporating isogeometric descriptions for the boundary in this 3D formulation achieves excellent accuracy in complex geometries, even with a reduced number of collocation points compared to classical description. As a result, this formulation exhibits strong agreement with experimental results [21].

The two-dimensional analyses via the aforementioned BEM/1D-BEM coupling address only cases where the reinforcements have a well-defined arrangement. Only the works with 3D formulations depict examples with random fiber distributions. Consequently, in those 2D examples, the user can manually control the discretization of the reinforcement domain. Conveniently, in 2D applications, the authors employ fully or partially uniform discretization models. This study presents an efficient discretization methodology, leveraging expected high-gradient adherence force results at the ends of the reinforcements. Another aspect addressed concerns the possibility of nearly singular integrals involving fiber domains when randomly arranged. The likelihood of impact on analysis accuracy is considerably higher in two-dimensions, making it important to investigate alternatives for mitigation. This study also proposes a methodology for that purpose.

2 Formulation

The coupling formulation used for BEM/1D-BEM is based on displacement compatibility between the matrix and the reinforcement. Considering the reinforcement as a slender domain Ω^f, it can be assumed, without significant loss of accuracy, that its behavior is analogous of a truss element. Therefore, Ω_f is one-dimensional. The coupling mechanism occurs through a adherence force distributed longitudinally along Ω^f. Figure 1 illustrates this behavior. By enforcing the equilibrium along the fiber domain interface, $\vec{f}^d = -\vec{f}^f$, where the first denotes the force Ω^f exercises on the matrix domain Ω, and the second represents the force Ω exercises on Ω^f.

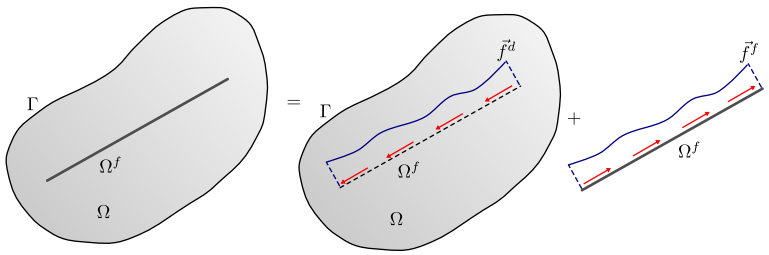


Figure 1. Thin reinforcement on a domain

Considering a source position in Ω, the Somigliana Identity, or boundary integral equation, for this problem reads as

$$u_k(s) + \int_\Gamma u_l(\Gamma)\, p^*_{kl}(s,\Gamma)\, d\Gamma = \int_\Gamma p_i(\Gamma)\, u^*_{ki}(s,\Gamma)\, d\Gamma + \sum_{f=1}^{nf} \int_{\Omega_f} f^d_i\left(\Omega^f\right) u^*_{ki}\left(s,\Omega^f\right) d\Omega^f. \tag{1}$$

One can apply a limiting process of the previous equation for source positions on the boundary Γ of Ω. The result is

$$\frac{1}{2}\delta_{kl}u_l\left(s\right)+\int\limits_{\Gamma}u_l\left(\Gamma\right)p_{kl}^{*}\left(s,\Gamma\right)d\Gamma=\int\limits_{\Gamma}p_i\left(\Gamma\right)u_{ki}^{*}\left(s,\Gamma\right)d\Gamma+\sum_{f=1}^{nf}\int\limits_{\Omega_f}f_i^d\left(\Omega^f\right)u_{ki}^{*}\left(s,\Omega^f\right)d\Omega^f. \tag{2}$$

In eqs. (1) and (2), indexes i, k, and l denote analysis dimensions. Terms $\vec{u}$ and $\vec{p}$ represent displacement and traction functions on Γ, respectively. Tensors U^* and P^* denote these functions from the Kelvin Fundamental Solution. The sums run over the number of fibers nf in Ω.

In the context of a two-dimensional analysis, eq. (1) provides 2 equations per source used in the discretization of the reinforcement domains. Each of these sources has 4 unknowns, which correspond to displacement and adherence force components. Equation (2) provides 2 equations for each source positioned on Γ. These sources also present 4 unknowns each, representing displacement and surface traction components. To solve the Boundary Value Problem (BVP), 2 of these unknowns must have prescribed values. Thus, eq. (2) is self-sufficient as expected. However, 2 more equations per source are required to form a square system of equations. The mechanical description of the fibers by the 1D-BEM provides these equations. Its boundary integral equation, valid for the longitudinal direction, is written as

$$u\left(s\right)+u\left(\Gamma^f\right)\,N^*\left(s,\Gamma^f\right)\Big|_{x^1}^{x^2}=N\left(\Gamma^f\right)u^*\left(s,\Gamma^f\right)\Big|_{x^1}^{x^2}+\int\limits_{\Omega}f^f\left(\Omega^f\right)u^*\left(s,\Omega^f\right)d\Omega^f, \tag{3}$$

where u^* and N^* are, respectively, the displacement and normal force functions derived from a fundamental solution for axial displacements in bars [22]. Since the boundary Γ^f of the linear domain consists of just two points, only linear approximation of mechanical quantities is possible. Nevertheless, the approximation order can be increased by including internal point equations such as eq. (3). In these equations, the integral can be performed discretely in the Gauss space as

$$\int\limits_{\Omega}f^f\left(\Omega^f\right)u^*\left(s,\Omega^f\right)d\Omega^f=\int\limits_{-1}^{1}\phi^{\alpha}\left(\xi\right)f_{\alpha}^{f}u^*\left(s,\xi\right)J\left(\xi\right)d\xi, \tag{4}$$

where ϕ are Lagrange polynomial basis functions and J is the Jacobian of the transformation from the integration space with coordinate ξ to the real space. At internal sources, the function u^* in eq. (4) has C^0 continuity at the source application position. To increase numerical integration accuracy, it is advisable to apply a domain subdivision process [23].

To represent the behavior of a truss element, one can expand eq. (3) to include displacements in the transverse direction. The addition of zero rows and columns accomplishes this. Thus, one obtains

$$h_{ij}\,\overline{u}_j=g_{ij}\,\overline{f}_j+\overline{p}_i, \tag{5}$$

where the vector $\vec{\overline{p}}$ corresponds to the integrals in eq. 4, and the indexes i and j represent each degree of freedom of the domain. Premultiplying both sides by the matrix $\mathbf{g}$ and nullifying the external force vector $\vec{\overline{f}}$, one obtains

$$\overline{k}_{kj}\,\overline{u}_j={g_{ki}}^{-1}\,\overline{p}_i, \tag{6}$$

analogous to FEM systems in the local element reference frame. The transformation process to the global reference frame is also analogous to FEM. In this formulation, to ensure the solution provides domain forces only in the axial direction of the fiber domain, one adds a unit value to the diagonal terms of $\mathbf{g}^{-1}$ corresponding to the transverse displacement degrees of freedom.

As Lagrangian basis functions describe the domain of each reinforcement, the domain force integral terms in eqs. (1) and (2) take the discrete form

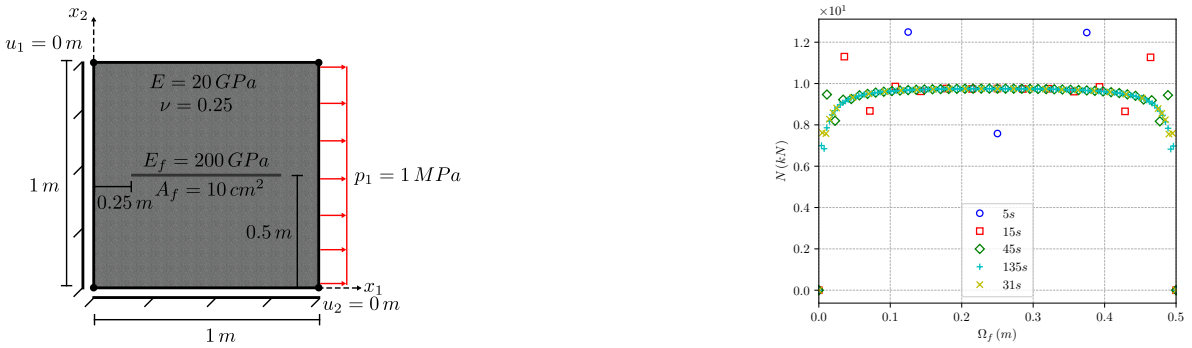
$$\sum_{f=1}^{nf} \int_{\Omega_f} f_i^d\left(\Omega_f\right)\, u_{ki}^*\left(s,\Omega_f\right)\, d\Omega_f = \sum_{fe=1}^{nfe} \int_{-1}^{1} \Phi_{ij}\left(\xi\right)\, f_j^d\left(f\right)\, u_{ki}^*\left(s,\xi\right)\, J\left(\xi\right)\, d\xi. \tag{7}$$

The indexes i and k represent the analysis dimensions, while the index j corresponds to each f^f component of the element sources. The tensor $\mathbf{\Phi}$ contains the distribution of the basis functions evaluated at the Gaussian coordinate. The sum takes over the total number of 1D-BEM domains used in the discretization. For the Γ discretization, the study employs the classical Lagrangian description and an isogeometric description based on NURBS curves.

3 Efficient discretization of thin reinforcements

The studies addressing the BEM/1D-BEM coupling utilize uniform or nearly uniform discretization models for the representation of reinforcements [16–21]. The adherence force results presents high gradients at its ends. This characteristic justifies the use of multiple elements for its discretization. From a computational viewpoint, each source used to describe an reinforcement domain requires integration of eqs. (1) and eqs. (2). Since the integration kernels are non-polynomial and tend to weak singularity, these integrations are computationally expensive. Moreover, each of these sources increases the global system of equations by 4 unknowns, potentially leading to high memory allocation.

An efficient way to discretize thin reinforcements consists of allocating a larger number of sources at its ends. Since the intention is to capture the expected high gradients and to provide a numerically smooth solution, linear elements satisfy the requirement at the extremities. Thus, a considerably more reasonable number of sources can precisely represent the remaining domain. Figure 2 illustrates the configuration of a simple example and the normal force results on the reinforcement obtained by different discretization models. In all models, a quadratic element describes each straight segment of Γ. Quadratic elements with same length describe Ω_f in the first four models ($5s$, $15s$, $45s$ and $135s$). In the last one ($31s$), 5 linear elements describe the first 5 centimeters of the reinforcement's end, while 10 quadratic elements describe its remaining. Clearly, the last discretization produces the desired numerical smoothing. Its results are as regular as those of the mesh using 135 equally spaced sources.



(a) (b)

Figure 2. Example of efficient thin reinforcement discretization: (a) configuration; (b) normal force on the reinforcement domain

4 Random disposition of fibers

In the context of BEM/1D-BEM applications, only 3D analyses depict properly domains with fibers randomly distributed [19, 20]. When placing sources in each fiber domain, near-singular integrals may occur if one of these sources lies very close to another domain or even to Γ. Therefore, it is necessary to take precautions regarding the crossing and overlapping of fiber domains. Due to the third coordinate in 3D analyses, such occurrences are considerably less likely than in 2D analyses. For the latter, the development of methodologies to mitigate these issues is advisable.

For crossing verification, this study computes a linear function $f : x_1 \to x_2$. Figure 3 illustrates this process. The index d corresponds to each position coordinate x. The superscript index consists of a letter and a number. The letter A designates an endpoint of the first domain, while the letter B indicates an endpoint of the second domain. The numbers correspond to the order of the points forming the line. Its function is only to facilitate the writing of the systems to calculate the coefficients of the functions. These systems are

$$\left\{ \begin{array}{c} a_0 \\ a_1 \end{array} \right\} = \begin{bmatrix} 1 & x_1^{A1} \\ 1 & x_1^{A2} \end{bmatrix}^{-1} \left\{ \begin{array}{c} x_2^{A1} \\ x_2^{A2} \end{array} \right\} \quad \text{and} \quad \left\{ \begin{array}{c} b_0 \\ b_1 \end{array} \right\} = \begin{bmatrix} 1 & x_1^{B1} \\ 1 & x_1^{B2} \end{bmatrix}^{-1} \left\{ \begin{array}{c} x_2^{B1} \\ x_2^{B2} \end{array} \right\}. \tag{8}$$

Once the coefficients are obtained, one can calculate the coordinates of the intersection point between the functions by

$$x_1^C = \frac{b_0 - a_0}{a_1 - b_1} \quad \text{or} \quad x_1^C = \frac{a_0 - b_0}{b_1 - a_1}. \tag{9}$$

As Fig. 4 illustrates, there is an intersection between two fiber domains if x_d^C belongs to both. When verifying this case within a tolerance, one discards the fiber to be inserted.

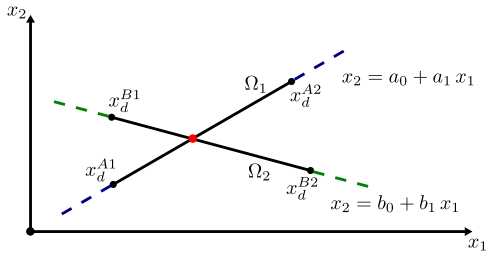


Figure 3. Functional geometric description for the fibers

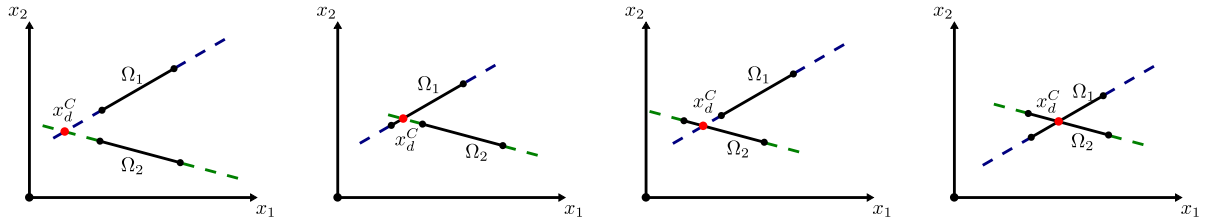
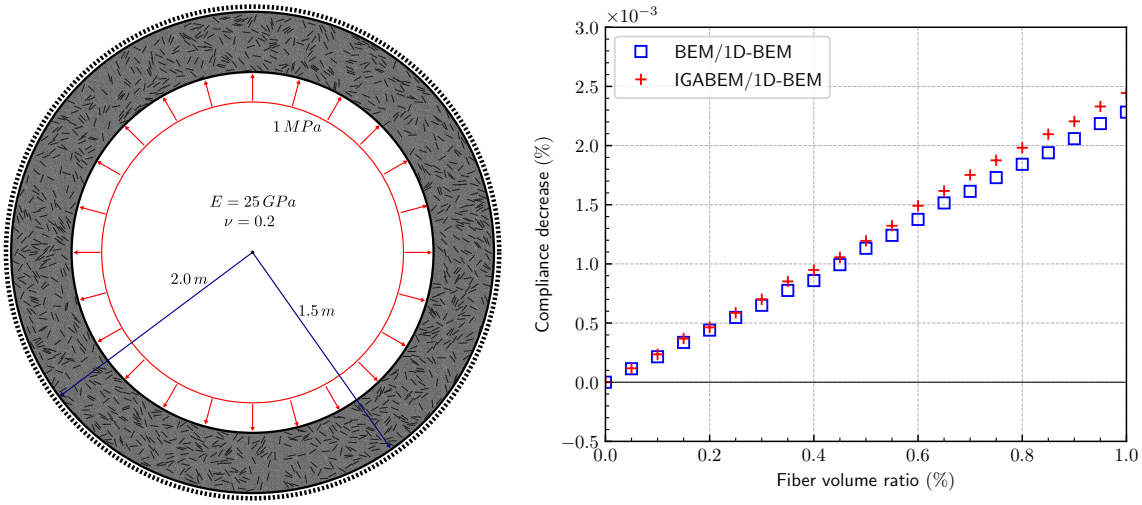


Figure 4. Crossing of fiber geometric functions: (a) $x_d^C \notin \Omega_1$ e $x_d^C \notin \Omega_2$; (b) $x_d^C \in \Omega_1$ e $x_d^C \notin \Omega_2$; (c) $x_d^C \notin \Omega_1$ e $x_d^C \in \Omega_2$; (d) $x_d^C \in \Omega_1$ e $x_d^C \in \Omega_2$

The verification of domain overlapping is mathematically more complex. In this study, for simplicity, it is assumed that the user prescribes a discretization model for all fibers. Thus, the distances between each source of the fiber to be inserted and all existing sources are verified. If any of these distances exceeds a predefined maximum value, one discards the fiber to be inserted.

This methodology is applied to an example with a ring-shaped geometry. Figure 5 illustrates its configuration for a 0.558% fiber volume ratio and the compliance results for the adopted models. In the classical BEM model, 24 quadratic elements describe Γ, while 8 NURBS describe it in the isogeometric model. The first point of each fiber is assigned a uniformly distributed probability in polar coordinates, i.e., $\mathbf{x}^p\,(r, \theta^p)$, with $r \sim U\,(1.5, 2.0)\ m$ and $\theta^p \in (0, 2\pi)$. A multi-objective optimization problem provides the geometric characteristics of the steel fibers [24]. The fiber volume ratio in Fig. 5(a) is one of its optimum results. According to a preliminary convergence analysis involving that ratio, 3 quadratic elements discretizing each fiber domain can provide enough accuracy

[23]. The results for compliance decrease as a function of fiber content are physically consistent and do not present significant accuracy issues. The difference in those provided by the two models consists in the Γ description. The classical BEM model approximates the Γ circular geometry by quadratic functions piecewise. In contrast, the IGABEM can describes those geometries with a computer numerical precision. The results in Fig. 5 also demonstrate the tendency on IGABEM model to provide greater compliance decrease with the increase of the fiber volume ratio.



(a) (b)

Figure 5. Example of random fiber disposition: (a) configuration; (b) compliance

5 Conclusions

This study addresses improved methodologies for discretizing thin reinforcements domains dispersed within a continuous medium, as well as alternatives to mitigate nearly-singular integrals in cases of random distribution of these domains. The discussions are conducted in the context of two-dimensional analyses using the BEM/1D-BEM coupling. The source clustering at the ends of the reinforcement domains has proven capable of producing a numerical smoothing of the adherence force function between the matrix and the embedded medium. The results demonstrate that this methodology can be effective, as it allows for a poorer mesh away from the ends. The success of the algorithm in avoiding fiber crossings is straightforward. However, it is hard to estimate the precision loss due to near-singularities throughout the process. The results regarding compliance decrease as a function of fiber content are physically consistent. Therefore, it can be inferred that such accuracy loss is not significant and that in the controlled distribution is effective.

The first author's master's dissertation presents further details regarding the formulation, more in-depth discussions on the scope of the present study, and additional examples [23].

Acknowledgements. This study was financed, in part, by the Coordenação de Aperfeiçoamento de Pessoal de Nível Superior – Brasil (CAPES) – Finance Code 001 and the São Paulo Research Foundation (FAPESP), Brasil - Process Number #2025/00921-6.

Authorship statement. The authors hereby confirm that they are the sole liable persons responsible for the authorship of this work, and that all material that has been herein included as part of the present paper is either the property (and authorship) of the authors, or has the permission of the owners to be included here.

References

[1] A. Naaman. Reinforced concrete. In K. J. Buschow, R. W. Cahn, M. C. Flemings, B. Ilschner, E. J. Kramer, S. Mahajan, and P. Veyssière, eds, *Encyclopedia of materials*, pp. 8095–8109. Elsevier, Oxford, 2001.

[2] D. Eyres and G. Bruce. Bulkheads and pillars. In D. Eyres and G. Bruce, eds, *Ship Construction*, chapter 18, pp. 207–223. Butterworth-Heinemann, Oxford, 7th ed edition, 2012.
[3] T. Megson. Structural components of aircraft. In T. Megson, ed, *Introduction to Aircraft Structural Analysis*, chapter 11, pp. 351–371. Butterworth-Heinemann, Boston, 2010.
[4] H. Coda, W. Venturini, and M. Aliabadi. A simple coupling of 2D BEM and FEM bar model applied to mass matrix elastodynamic analysis. *WIT Transactions on Modelling and Simulation*, vol. 18, pp. 1–10, 1997.
[5] H. Coda and W. Venturini. On the coupling of 3D BEM and FEM frame model applied to elastodynamic analysis. *International Journal of Solids and Structures*, vol. 36, n. 31, pp. 4789–4804, 1999.
[6] H. B. Coda, W. S. Venturini, and M. H. Aliabadi. A general 3D BEM/FEM coupling applied to elastodynamic continua/frame structures interaction analysis. *International Journal for Numerical Methods in Engineering*, vol. 46, n. 5, pp. 695–712, 1999.
[7] H. B. Coda. Dynamic and static non-linear analysis of reinforced media: a BEM/FEM coupling approach. *Computers & Structures*, vol. 79, n. 31, pp. 2751–2765, 2001.
[8] A. S. Botta and W. S. Venturini. Reinforced 2D domain analysis using BEM and regularized BEM/FEM combination. *Computer Modeling in Engineering & Sciences*, vol. 8, n. 1, pp. 15–28, 2005.
[9] F. C. da Rocha. Análise de domínios reforçados através da combinação MEC/MEF considerando modelos de aderência. Mestrado em engenharia civil (engenharia de estruturas), Escola de Engenharia de São Carlos, Universidade de São Paulo, São Carlos, 2009.
[10] F. C. da Rocha, W. S. Venturini, and H. B. Coda. Sliding frame-solid interaction using BEM/FEM coupling. *Latin American Jounal of Solids and Structures*, vol. 11, pp. 1376–1399, 2014.
[11] E. D. Leonel. *Modelos não lineares do Método dos Elementos de Contorno para análise de problemas de fratura e aplicação de modelos de confiabilidade e otimização em estruturas submetidas à fadiga*. Doutorado em engenharia de estruturas, Escola de Engenharia de São Carlos, Universidade de São Paulo, São Carlos, 2009.
[12] L. G. Leite, H. B. Coda, and W. S. Venturini. Two-dimensional solids reinforced by thin bars using the boundary element method. *Engineering Analysis with Boundary Elements*, vol. 27, n. 3, pp. 193–201, 2003.
[13] L. G. Leite and W. S. Venturini. Boundary element formulation for 2D solids with stiff and soft thin inclusions. *Engineering Analysis with Boundary Elements*, vol. 29, n. 3, pp. 257–267, 2005.
[14] K. Riederer, C. Duenser, and G. Beer. Simulation of linear inclusions with the bem. *Engineering Analysis with Boundary Elements*, vol. 33, n. 7, pp. 959–965, 2009.
[15] G. Beer, C. Dünser, E. Ruocco, and V. Mallardo. Efficient simulation of inclusions and reinforcement bars with the isogeometric boundary element method. *Computer Methods in Applied Mechanics and Engineering*, vol. 372, pp. 1–22, 2020.
[16] L. P. Buffon. Formulações do método dos elementos de contorno para a análise mecânica de domínios planos não-homogêneos enrijecidos. Mestrado em Engenharia Civil (engenharia de estruturas), Escola de Engenharia de São Carlos, Universidade de São Paulo, São Carlos, 2018.
[17] A. Rodrigues Neto. Modelos numéricos baseados no método dos elementos de contorno para a análise mecânica de domínios viscoelásticos enrijecidos com comportamento não-linear. Mestrado em engenharia civil (engenharia de estruturas), Escola de Engenharia de São Carlos, Universidade de São Paulo, São Carlos, 2019.
[18] A. Rodrigues Neto and E. D. Leonel. The mechanical modelling of nonhomogeneous reinforced structural systems by a coupled BEM formulation. *Engineering Analysis with Boundary Elements*, vol. 109, pp. 1–18, 2019.
[19] A. Rodrigues Neto and E. D. Leonel. Three dimensional nonlinear BEM formulations for the mechanical analysis of nonhomogeneous reinforced structural systems. *Engineering Analysis with Boundary Elements*, vol. 123, pp. 200–219, 2021.
[20] A. Rodrigues Neto. *Numerical formulations based on the Isogeometric Boundary Element Method for the mechanical analysis of three-dimensional reinforced nonhomogeneous solids*. PhD in Civil Engineering (Structural Engineering), São Carlos School of Engineering, University of São Paulo, São Carlos, 2023.
[21] A. Rodrigues Neto and E. D. Leonel. Nonlinear IGABEM formulations for the mechanical modelling of 3D reinforced structures. *Applied Mathematical Modelling*, vol. 102, pp. 62–100, 2022.
[22] P. Banerjee and R. Butterfield. *Boundary Element Methods in Engineering Science*. McGraw-Hill, Maidenhead, 1981.
[23] M. S. O. César Filho. Contribuições à análise de estruturas enrijecidas e à otimização topológica utilizando o método dos elementos de contorno. Mestrado em Engenharia Civil (Engenharia de Estruturas), Escola de Engenharia de São Carlos, Universidade de São Paulo, São Carlos, 2025.
[24] F. Bayramov, C. Taşdemir, and M. Taşdemir. Optimisation of steel fibre reinforced concretes by means of statistical response surface method. *Cement and Concrete Composites*, vol. 26, n. 6, pp. 665–675, 2004.